Min Yuan, Bing-xin Yang, Yi-de Ma, Jiu-wen Zhang, Fu-xiang Lu, Tong-feng Zhang, 2015. Multi-scale UDCT dictionary learning based highly undersampled MR image reconstruction using patch-based constraint splitting augmented Lagrangian shrinkage algorithm. *Frontiers of Information Technology & Electronic Engineering*, **16**(12):1069-1087. [doi:10.1631/FITEE.1400423]

Multi-scale UDCT dictionary learning based highly undersampled MR image reconstruction using patch-based constraint splitting augmented Lagrangian shrinkage algorithm

Front Inform Technol & Electron Eng

Key words: Compressed sensing (CS), Magnetic resonance imaging (MRI), Uniform discrete curvelet transform (UDCT), Multi-scale dictionary learning (MSDL), Patch-based constraint splitting augmented Lagrangian shrinkage algorithm (PB C-SALSA)

Contact: Min Yuan
E-mail: yuanm@lzu.edu.cn

ORCID: http://orcid.org/0000-0001-7855-8678

Motivation

- By adopting both multi-scale and learning point-of-views, incorporating the superior multi-scale properties of UDCT with the data matching adaptability of trained dictionaries, a flexible sparsity framework was proposed to allow sparser representation and prominent hierarchical essential features capture for MR images so as to substantially improve reconstruction performance for CS-MRI.

Front Inform Technol & Electron Eng

Main ideas

- Multi-scale decomposition is implemented by using UDCT due to its prominent properties of lower redundancy ratio, hierarchical data structure, and ease of implementation. Each sub-dictionary of different sub-bands is trained independently to form the multi-scale dictionaries.

- Corresponding to this brand-new sparsity model, constraint splitting augmented Lagrangian shrinkage algorithm (C-SALSA) is modify as patch-based C-SALSA (PB C-SALSA) to solve the constraint optimization problem of regularized image reconstruction.

Front Inform Technol & Electron Eng

Framework of our method

- The flowchart of the proposed UDPC

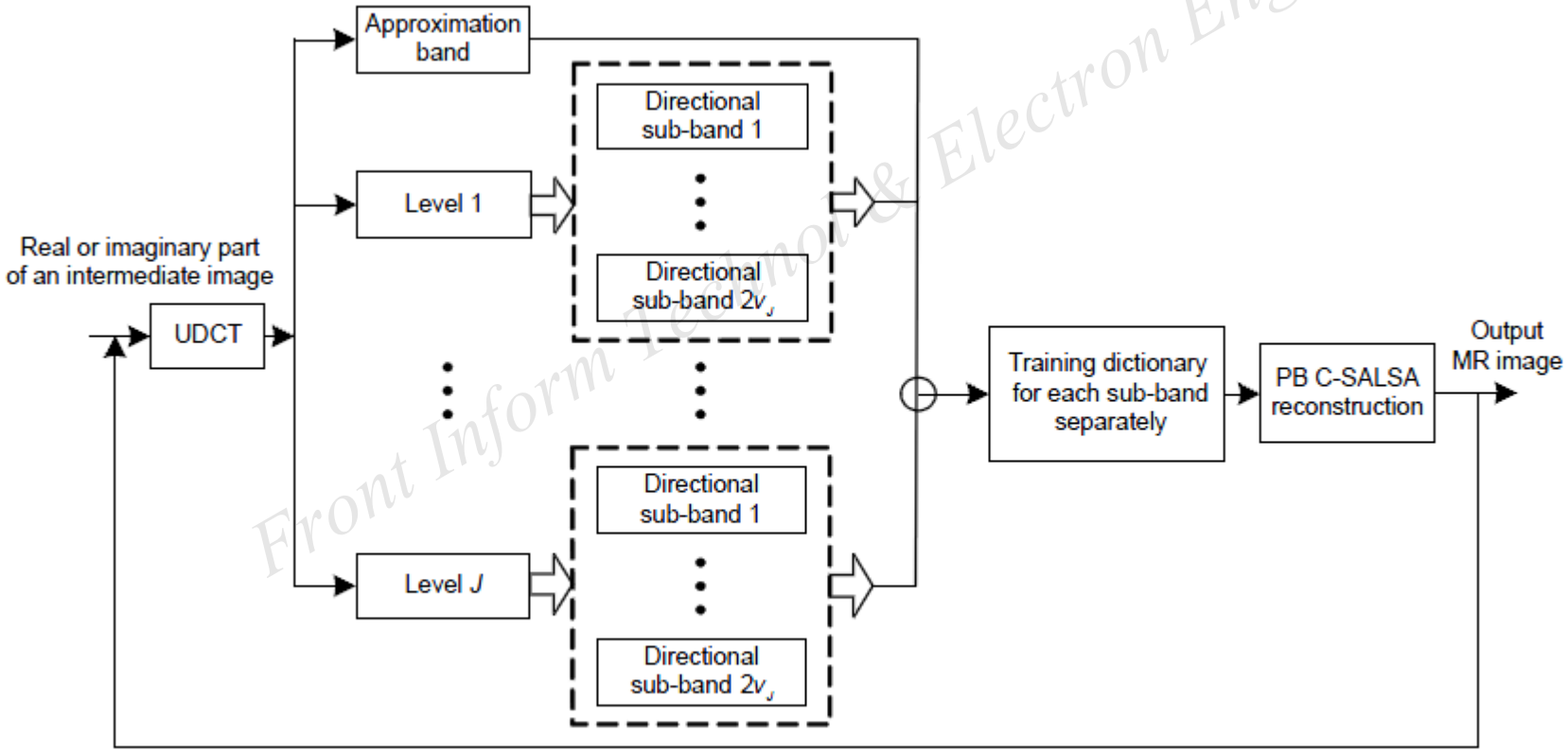

Front Inform Technol & Electron Eng

Fig. 2 Flowchart of the proposed UDPC-based MRI reconstruction

Method (I)

- UDCT DL

Algorithm 1 Multi-scale UDCT dictionary learning (MS UDCT DL) for solving sub-problem (7)

Require: the sample data applied to train multi-scale dictionary $\boldsymbol{x}$, the number of decomposition levels J, the number of atoms per sub-dictionary K, the size of atoms in each sub-dictionary n, UDCT operator $\boldsymbol{\Psi}$, scale indicator v_J

1: Initialize multi-scale dictionary: use the UDCT to decompose the initial image into $B=J\times 2v_J+1$ sub-bands. Set each initial sub-dictionary $\boldsymbol{D}_b \in \mathbb{C}^{n\times K}$ ($b=1, 2, \ldots, B$) to the combination of left singular vectors of the corresponding UDCT coefficient sub-bands using singular value decomposition and some random columns of training coefficient matrix

2: **for** $b=1, 2, \ldots, B$ **do**

3: Divide $(\boldsymbol{\Psi x})_b$ to maximum overlapped patches $\sum_{ij}\widetilde{\mathbf{coef}_{ij}}$, where coefficient patch $\widetilde{\mathbf{coef}_{ij}} = \boldsymbol{R}_{ij}(\boldsymbol{\Psi x})_b$ is denoted as a column vector of size $n\times 1$

4: Arrange $\sum_{ij}\widetilde{\mathbf{coef}_{ij}}$ in a row vector sequentially

5: Extract a fraction column of $\sum_{ij}\widetilde{\mathbf{coef}_{ij}}$ randomly

6: Apply the K-SVD algorithm to the random partial columns of $\sum_{ij}\widetilde{\mathbf{coef}_{ij}}$ to train each sub-dictionary $\boldsymbol{D}_b$, separately

7: **end for**

8: **Return** set $\boldsymbol{D}$ of all sub-dictionaries $\boldsymbol{D}_b \in \mathbb{C}^{n\times K}$ ($b=1, 2, \ldots, J\times 2v_J+1$)

Front Inform Technol & Electron Eng

Method (II)

- The flowchart of PB C-SALSA reconstruction

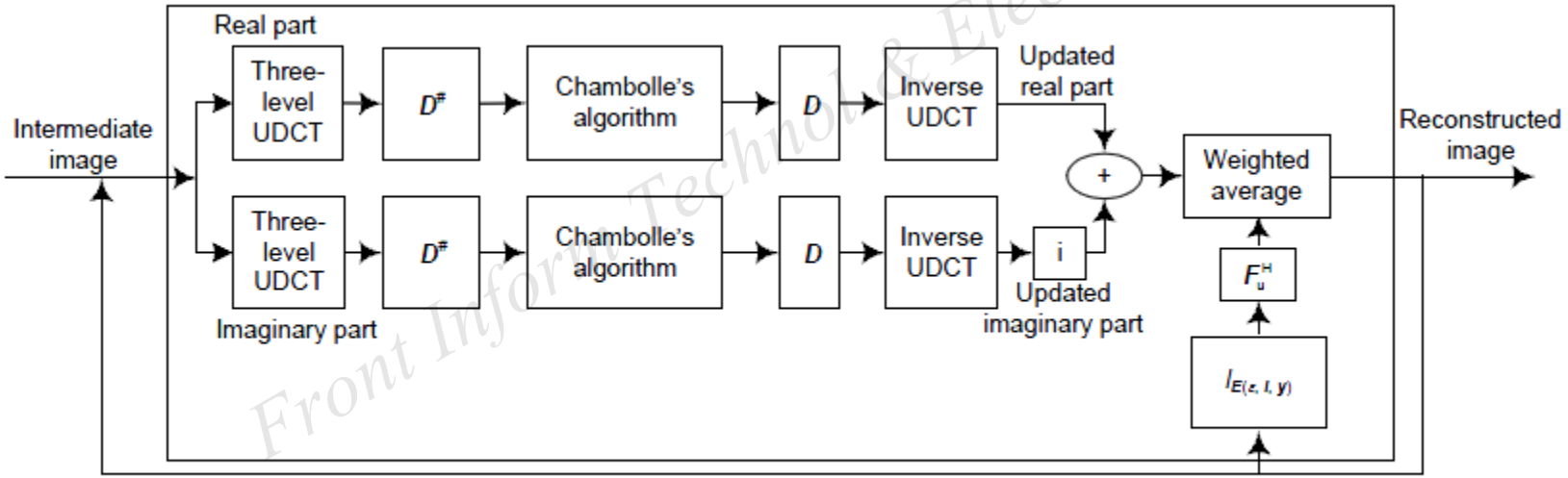

Fig. 3 Patch-based constraint splitting augmented Lagrangian shrinkage algorithm reconstruction

Front Inform Technol & Electron Eng

Method (III)

- PB C-SALSA reconstruction

Algorithm 2 MS UDCT DL based MR image reconstruction by PB C-SALSA (UDPC) for solving problem (8)

Require: k-space data $\boldsymbol{y}$, the undersampled Fourier operator $\boldsymbol{F}_{\mathrm{u}}$, and UDCT operator $\boldsymbol{\Psi}$

1: Set $\boldsymbol{x}_0 = \boldsymbol{F}_{\mathrm{u}}^{\mathrm{H}}\boldsymbol{y}$, $k=0$, and choose $\lambda>0$, $J=3$, $2v_j=6$, $B=J\times 2v_j+1$, $r=1$ or 2 ($r=1, 2$ denotes the real and imaginary parts of an image, respectively). The initial representation coefficient of the UDCT sub-band over sub-dictionary $\boldsymbol{D}_b$ is denoted as $\boldsymbol{u}_0^{(r)}$:

$$\boldsymbol{u}_0^{(r)} = \left\{\boldsymbol{u}_{0b}^{(r)}\right\} = \left\{(\boldsymbol{D}_b^{(r)})^{\#}(\boldsymbol{\Psi}\boldsymbol{x}_0^{(r)})_b \mid b=1,2,\cdots,B\right\},$$

$$\boldsymbol{v}_0 = \boldsymbol{y},\ \Delta\boldsymbol{u}_0^{(r)} = \boldsymbol{0}\times\boldsymbol{u}_0^{(r)},\ \Delta\boldsymbol{v}_0 = \boldsymbol{0}\times\boldsymbol{v}_0,$$

where $\boldsymbol{u}_{0b}^{(r)}$ denotes the coefficients in terms of sub-dictionary $\boldsymbol{D}_b$, $(\boldsymbol{\Psi}\boldsymbol{x}_0^{(r)})_b$ denotes the sub-band coefficients of $\boldsymbol{\Psi}\boldsymbol{x}_0^{(r)}$, and the set of all sub-dictionaries is

$$\boldsymbol{D}^{(r)} = \left\{\boldsymbol{D}_b^{(r)} \mid b=1,2,\cdots,B,\ r=1,2\right\}$$

2: **Repeat**

3: $$\boldsymbol{s}_k = \boldsymbol{\Psi}^{\mathrm{H}}\boldsymbol{D}^{(1)}(\boldsymbol{u}_k^{(1)}+\Delta\boldsymbol{u}_k^{(1)}) + \mathrm{li}\times\boldsymbol{\Psi}^{\mathrm{H}}\boldsymbol{D}^{(2)}(\boldsymbol{u}_k^{(2)}+\Delta\boldsymbol{u}_k^{(2)}) + \boldsymbol{F}_{\mathrm{u}}^{\mathrm{H}}(\boldsymbol{v}_k+\Delta\boldsymbol{v}_k)$$

4: $$\boldsymbol{x}_{k+1} = \left[\sum_{r=1}^{2}(\boldsymbol{\Psi}^{\mathrm{H}}\boldsymbol{D}^{(r)})(\boldsymbol{D}^{(r)})^{\#}(\boldsymbol{\Psi}\boldsymbol{x}) + \boldsymbol{F}_{\mathrm{u}}^{\mathrm{H}}\boldsymbol{F}_{\mathrm{u}}\right]^{-1}\boldsymbol{s}_k$$

5: **for** $b=1, 2, \ldots, B$ **do**

6: **for** $r=1, 2$ **do**

7: Moreau proximal mapping function of $\boldsymbol{u}_b^{(r)}$:

$$\boldsymbol{u}_{(k+1)b}^{(r)} = \boldsymbol{\Theta}_{\lambda\phi}[(\boldsymbol{D}_b^{(r)})^{\#}(\boldsymbol{\Psi}\boldsymbol{x}_{k+1}^{(r)})_b - \Delta\boldsymbol{u}_{kb}^{(r)}]$$

8: $$\Delta\boldsymbol{u}_{(k+1)b}^{(r)} = \Delta\boldsymbol{u}_{kb}^{(r)} - (\boldsymbol{D}_b^{(r)})^{\#}(\boldsymbol{\Psi}\boldsymbol{x}_{k+1}^{(r)})_b + \boldsymbol{u}_{(k+1)b}^{(r)}$$

9: **end for**

10: **end for**

11: Assemble all $\boldsymbol{u}_{(k+1)b}^{(r)}$ to form the updated $\boldsymbol{u}_{(k+1)}^{(r)}$, and assemble all $\Delta\boldsymbol{u}_{(k+1)b}^{(r)}$ to form the updated $\Delta\boldsymbol{u}_{(k+1)}^{(r)}$

12: Moreau proximal mapping function of $\boldsymbol{v}$:

$$\boldsymbol{v}_{k+1} = \boldsymbol{\Theta}_{l_{E(\varepsilon,I,y)}}(\boldsymbol{F}_{\mathrm{u}}\boldsymbol{x}_{k+1} - \Delta\boldsymbol{v}_k)$$

13: $$\Delta\boldsymbol{v}_{k+1} = \Delta\boldsymbol{v}_k - \boldsymbol{F}_{\mathrm{u}}\boldsymbol{x}_{k+1} + \boldsymbol{v}_{k+1}$$

14: $k \leftarrow k+1$

15: **Until** some stopping criterion is satisfied

16: **Return** $\hat{x}$

Front Inform Technol & Electron Eng

Major results (I)

Water phantom

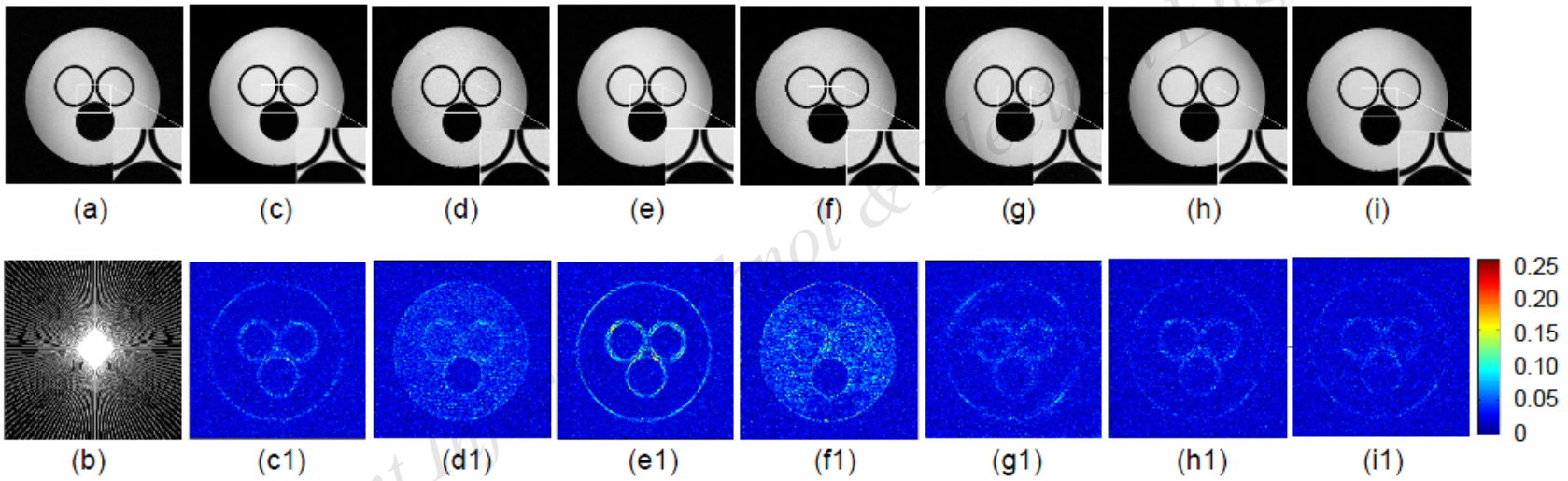

Fig. 4 Comparison of reconstruction results for a water phantom

(a) Fully sampled water phantom (256×256); (b) Simulated *k*-space trajectory (pseudo-radial lines mask with 25.97% sampling rate); (c)–(i) Reconstruction using LDP, wav_CSALSA, DLMRI, PBDW, PBDWS, PANO, and the proposed UDPC, respectively; (c1)–(i1) Magnitudes of reconstruction errors for (c)–(i) with the scale of [0, 0.25], respectively

Major results (II)

CS phantom

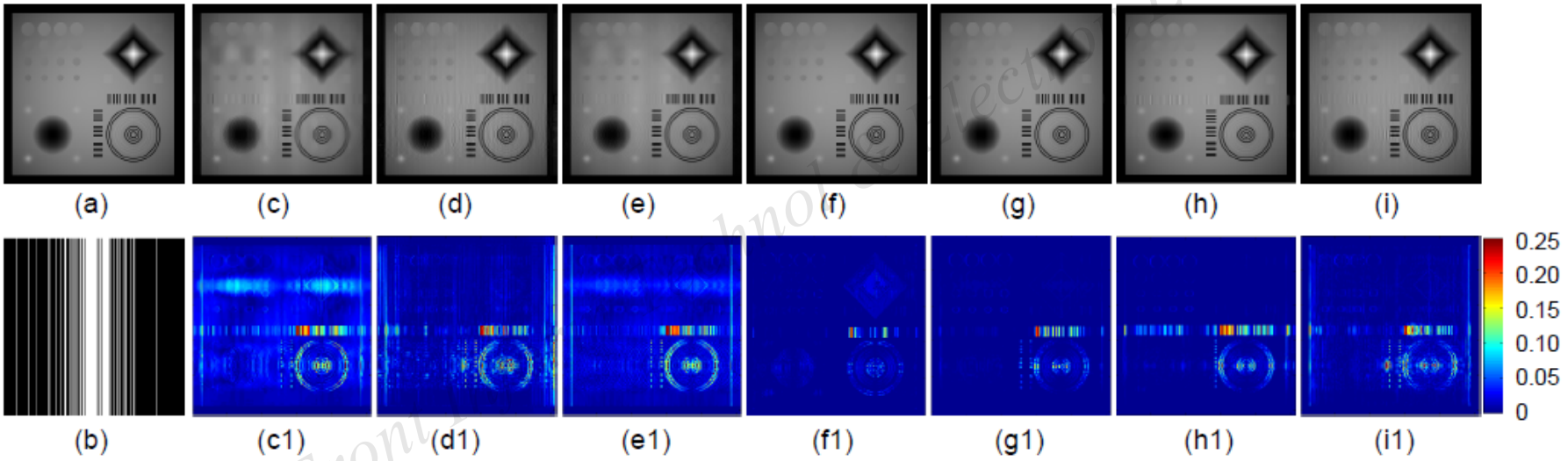

Fig. 5 Comparison of reconstructions using different methods for CS phantom

(a) Reference CS phantom image (256×256); (b) Cartesian sampling mask with sampling rate 25%; (c)–(i) Reconstruction using LDP, wav_CSALSA, DLMRI, PBDW, PBDWS, PANO, and UDPC, respectively; (c1)–(i1) Magnitudes of reconstruction errors for (c)–(i) with the scale of [0,0.25], respectively

Major results (III)

T2-weighted image of the brain

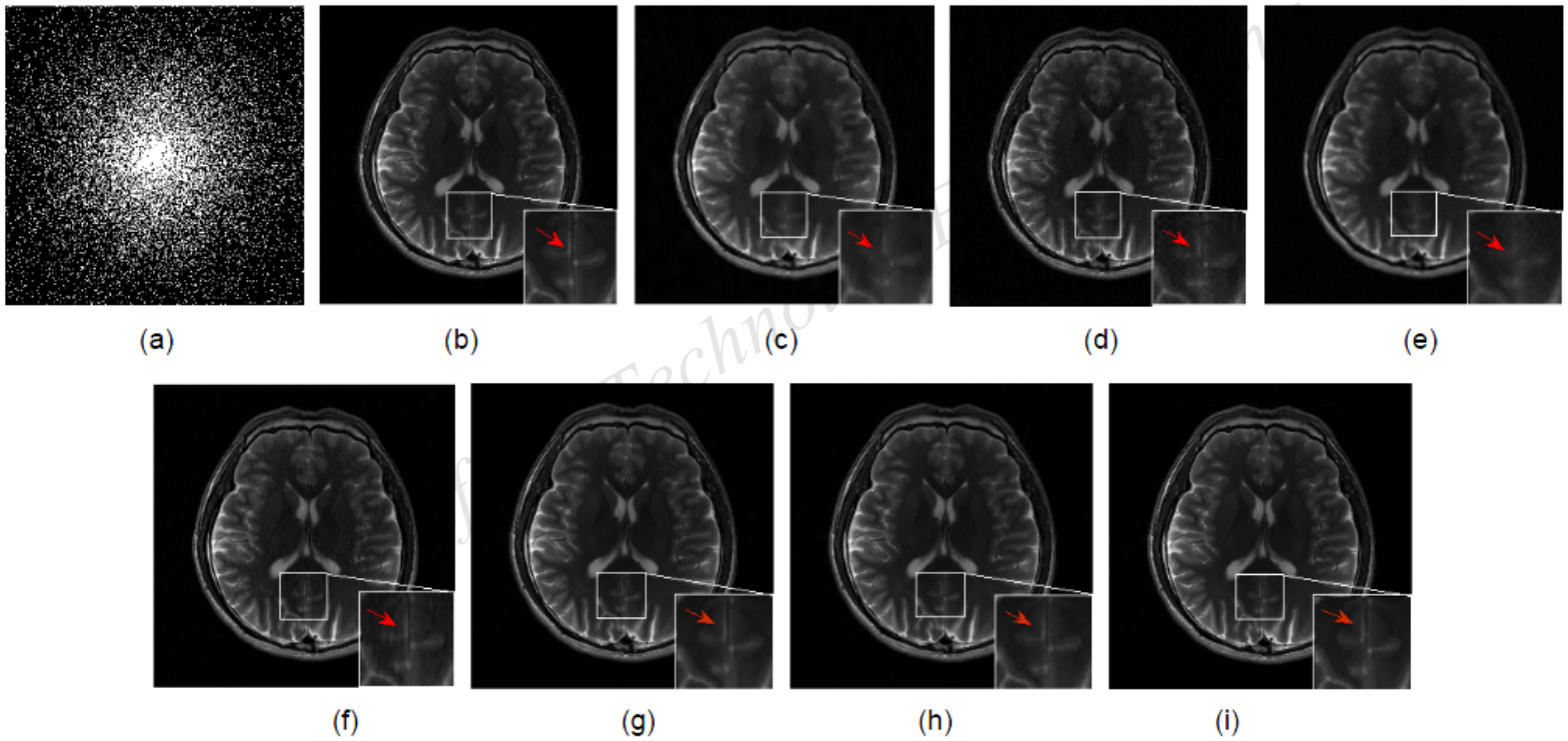

Fig. 6 Comparison of reconstruction results for the T2-weighted brain image

(a) Variable density random sampling pattern with sampling rate 20.05%; (b) Reconstructed image from fully sampled data (256×256); (c)–(i) Reconstruction using LDP, wav_CSALSA, DLMRI, PBDW, PBDWS, PANO, and the proposed UDPC, respectively

Major results (IV)

Noisy T2-weighted brain image data

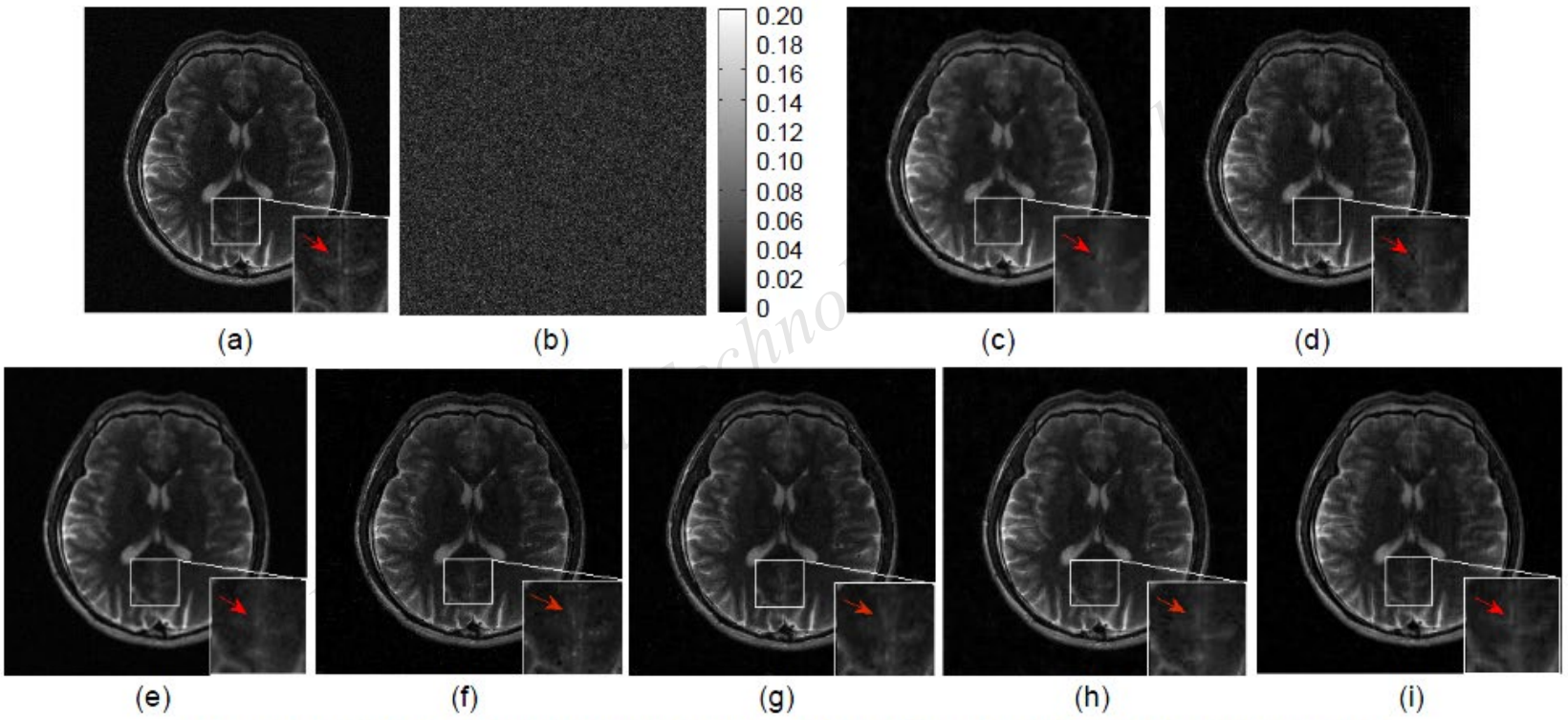

Fig. 7 Comparison of reconstruction results for noisy T2-weighted brain image data

(a) Reconstructed image from fully sampled noisy data (σ=10.2); (b) Noise magnitude in (a); (c)–(i) Reconstruction using LDP, wav_CSALSA, DLMRI, PBDW, PBDWS, PANO, and the proposed UDPC, respectively

Major results (V)

Table 1 Comparison of the objective assessment indices of CS-MRI reconstruction for noise-added data via UDPC to compared methods using three different sampling patterns with different sampling rates*

Method	T2-weighted brain image & mask_VDRS_2001 & sigma=10.2				Water phantom & mask_PRS_2597 & sigma=6.5				CS phantom & mask_Carteian_25 & sigma=6.5			
	PSNR (dB)	TEI	SSIM	RLNE	PSNR (dB)	TEI	SSIM	RLNE	PSNR (dB)	TEI	SSIM	RLNE
LDP	30.25	0.52	0.79	0.19	33.57	0.68	0.72	0.04	29.04	0.57	0.88	0.09
wav_CSALSA	29.41	0.52	0.71	0.21	16.94	0.50	0.65	0.30	28.65	0.58	0.74	0.09
DLMRI	30.36	0.51	0.86	0.19	32.73	0.66	0.73	0.05	31.45	0.66	0.84	0.07
PBDW	30.01	0.57	0.77	0.19	31.43	0.66	0.70	0.06	33.33	0.68	0.87	0.05
PBDWS	31.65	0.61	0.79	0.16	34.20	0.68	0.81	0.04	33.35	0.71	0.88	0.05
PANO	31.47	0.61	0.77	0.16	34.46	0.69	0.82	0.04	32.20	0.69	0.87	0.06
UDPC	31.56	0.60	0.86	0.16	33.52	0.68	0.78	0.04	32.11	0.69	0.87	0.06

* mask_VDRS_2001 denotes variable density random sampling mask with 20.01% sampling rate, mask_ PRS_2597 denotes pseudo radial lines sampling mask with 25.97% sampling rate, and mask_Carteian_25 denotes with variable density (Cartesian sampling mask in *k*-space with 25% sampling rate)

Table 2 Comparisons of Lin's CCC values of each reconstruction method with respect to the full sampling result for phantom and in vivo reconstructions

Method	Lin's CCC value			
	Water phantom	CS phantom	T2-weighted brain image	Noisy T2-weighted brain image
LDP	0.9984	0.9849	0.9796	0.9430
wav_CSALSA	0.9120	0.9880	0.9868	0.9408
DLMRI	0.9981	0.9885	0.9746	0.9485
PBDW	0.9981	0.9888	0.9887	0.9489
PBDWS	0.9985	0.9902	0.9901	0.9516
PANO	0.9988	0.9930	0.9904	0.9525
UDPC	0.9988	0.9932	0.9904	0.9535

Front Inform Technol & Electron Eng

Conclusions

- A novel multi-scale UDCT dictionary learning framework was proposed for CS reconstruction of MR data.
  - A complex-valued multi-scale dictionary was trained to sparsely represent complex-valued data, which helps remove aliasing and Gibbs ringing artifacts and to preserve rich intrinsic properties of MR image.
  - Patch-based C-SALSA enforces data fidelity with a rapid convergence speed without degrading the reconstruction quality.

- The proposed method can provide superior reconstruction performance at high acceleration rates with or without noise, which leads to greatly improved visual quality of the reconstruction image with much less graininess and less information loss than the others.

Front Inform Technol & Electron Eng